9-15-1991

Temperature dependence of optical properties of GaAs

Huade Yao
University of Nebraska - Lincoln

Paul G. Snyder
University of Nebraska - Lincoln, psnyder1@unl.edu

John A. Woollam
University of Nebraska - Lincoln

Temperature dependence of optical properties of GaAs

Huade Yao, Paul G. Snyder, and John A. Woollam
University of Nebraska, Center for Microelectronic and Optical Materials Research,
and Department of Electrical Engineering, Lincoln, Nebraska 68588-0511

Pseudodielectric functions $\langle \epsilon \rangle = \langle \epsilon_1 \rangle + i \langle \epsilon_2 \rangle$ of GaAs were measured by spectroscopic ellipsometry (SE), in the range of 1.6–4.45 eV, at temperatures from room temperature (RT) to ~610 °C. A very clean, smooth surface was obtained by first growing an epitaxial layer of GaAs on a GaAs substrate and immediately capping it with a protective layer of arsenic. The cap prevented surface oxidation during transport to the measurement chamber, where it was evaporated under ultrahigh vacuum at ~350 °C. Room-temperature SE results from this surface are in good agreement with those in the literature obtained by wet-chemical etching. A quantitative analysis of the $\langle \epsilon \rangle$ spectrum was made using the harmonic-oscillator approximation (HOA). It is shown by the HOA that the E_1 and $E_1 + \Delta_1$ energy-band critical points shift downward ~300 meV as temperature increases from RT to ~610 °C. An algorithm was developed, using the measured optical constants at a number of fixed temperatures, to compute the dielectric function spectrum at an arbitrary temperature in the range of 22–610 °C. Therefore, the ellipsometer can be utilized as an optical thermometer to determine the sample surface temperature.

I. INTRODUCTION

Spectroscopic ellipsometry[1] (SE) is a nondestructive optical measurement, which is attractive for *in situ* growth monitoring. SE has demonstrated high sensitivity to layer thicknesses and compositions, in *ex situ* measurements of GaAs-Al$_x$Ga$_{1-x}$As heterostructures.[2–4] In fact, SE is very sensitive to *any* physical property or process (e.g., temperature, oxide desorption, etc.) which affects the optical constants and/or surface or interface conditions. In the past, *in situ* SE has been used to monitor growth of GaAs-AlGaAs structures in a metalorganic vapor-phase epitaxy chamber.[5,6] More recently, real-time SE measurements of molecular-beam epitaxial (MBE) growth have been performed.[7,8] In order to convert the highly sensitive raw data into quantitative information, a model is needed to fit the data. The model should account for the multilayer structure, with parameters for the thickness and composition of each layer, interfacial and surface roughness or intermixing, and temperature dependence of the optical contents (dielectric function ϵ) for each material. SE data of GaAs as a function of temperature were previously obtained and analyzed,[9] from -253 to 477 °C. However, these data were measured from an oxidized GaAs surface. The effect of the oxide layer was mathematically removed, by assuming that its thickness and optical constants remained constant throughout the entire temperature range. This latter assumption is incorrect at higher temperatures,[7,10,11] where the oxide reacts with the substrate. Inevitably, the accuracies of the ϵ magnitudes determined in such an analysis must suffer, although the critical-point-energy analysis was probably less affected. Thus we felt it was necessary to measure an oxide-free surface, to minimize errors due to surface overlayers and their evolution with temperature. In addition, the existing SE data for GaAs does not include the temperature range up to typical MBE-growth temperatures (~600 °C), an important aspect for *in situ* growth monitoring and control.

Here, we report SE-measured pseudodielectric functions and related optical constants of GaAs, measured directly from a very clean bulk-GaAs surface, in the range of 1.6–4.45 eV at temperatures from room temperature (RT) to ~610 °C in increments of approximately 50 °C. A harmonic-oscillator approximation (HOA) was fitted to these data. This model differs from the critical-point model, used previously to fit similar data.[9,12] Our primary purpose in using HOA analysis is to provide a simple and accurate means of analytically reproducing the measured $\epsilon(h\nu,T)$ spectra.

II. THEORY AND ANALYSIS

The spectroscopic ellipsometer is designed to accurately determine the values of $\tan(\psi)$ and $\cos(\Delta)$, which are the amplitude and projected phase of the complex ratio

$$\rho = R_p / R_s = \tan(\psi) e^{i\Delta}, \tag{1}$$

where R_p and R_s are the complex reflectances of light polarized parallel to (p) or perpendicular to (s) the plane of incidence. The results of the SE experimental measurements can be expressed as $\psi(h\nu_i, \Phi_j)$ and $\Delta(h\nu_i, \Phi_j)$, where $h\nu$ is the photon energy and Φ is the external angle of incidence. The ψ and Δ are sensitive to changes of the surface conditions, overlayer thicknesses, dielectric functions, and other parameters of the sample.[2,13]

The pseudodielectric function $\langle \epsilon \rangle$ is obtained from the ellipsometrically measured values of ρ, in a two-phase model (ambient/substrate):[13]

$$\langle \epsilon \rangle = \langle \epsilon_1 \rangle + i \langle \epsilon_2 \rangle$$
$$= \epsilon_a \left[\left(\frac{1-\rho}{1+\rho} \right)^2 \sin^2 \Phi \tan^2 \Phi + \sin^2 \Phi \right], \tag{2}$$

regardless of the possible presence of surface overlayers. The ϵ_a in Eq. (2) represents the ambient dielectric function (i.e., $\epsilon_a = 1$ in vacuum). It has been shown[14,15] that the peak value of the imaginary part $\langle\epsilon_2\rangle$, which corresponds to the critical point E_2 position (i.e., ~ 4.8 eV for GaAs at RT), is readily interpretable: The highest value relates to the cleanest and smoothest surface. Decreasing values of $\langle\epsilon_2\rangle$ indicate surface degradation: i.e., the presence of surface oxide or other overlayers, microscopic roughness or porosity in the near surface region, etc. In addition, the penetration depth of light at the E_2 position (e.g., ~ 55 Å for GaAs at RT) is nearly minimized so that the surface effects are maximized. Therefore, the ellipsometric probe at or near the E_2 position is a sensitive test of the surface condition of semiconductors.

The dielectric response of a solid crystal can be quantum mechanically expressed as a superposition of a set of harmonic oscillators.[16,17] It is given by

$$\epsilon(E,\Gamma) = 1 + \frac{\hbar^2 e^2}{\pi^2 m^2 E^2} \int_{BZ} d^3k \, |\hat{e}\cdot\mathbf{P}_{cv}(k)|^2$$
$$\times \left(\frac{1}{E + E_{cv}(k) + i\Gamma} - \frac{1}{E - E_{cv}(k) + i\Gamma}\right), \quad (3)$$

where $\mathbf{P}_{cv}(k) = \langle ck|\mathbf{p}|vk\rangle$ is the momentum matrix element, c and v refer to conduction and valence bands, respectively, $\hat{e}$ is the unit polarization vector of the photon electric field, $E_{cv} = E_c(k) - E_v(k)$ is the interband transition energy, Γ is the broadening parameter, and the integral is over the Brillouin zone.

Erman et al.[17] applied the above theory to analyze SE data from semiconductors. Instead of doing the complicated integrals, a summation of seven harmonic oscillators representing energy-band critical-point transitions in the range of measurements were used to reduce the total number of oscillators. We also found that a seven-oscillator model could fit our experimental data to a satisfactory degree. Therefore, the dielectric function can be written as

$$\epsilon(E) = 1 + \sum_{k=1}^{7} A_k \left(\frac{1}{E + E_k + i\Gamma_k} - \frac{1}{E - E_k + i\Gamma_k}\right). \quad (4)$$

A detailed description of our data analysis by using this harmonic-oscillator approximation will be represented in Sec. IV.

If the sample contains one or more overlayers, the SE data must be numerically fitted. A model is assumed, for example, a three-phase model: ambient/oxide/substrate, and $\psi^c(h\nu_i,\Phi_j)$ and $\Delta^c(h\nu_i,\Phi_j)$ are calculated as in Eq. (1) for comparison with the measured values. A regression analysis is used to vary the model parameters (e.g., oxide thickness or dielectric function) until the calculated and measured values match as closely as possible. This is done by minimizing the mean-square error (MSE) function, defined as

$$\text{MSE} = \frac{1}{N} \sum_{i,j} \{ [\psi(h\nu_i,\Phi_j) - \psi^c(h\nu_i,\Phi_j)]^2 +$$
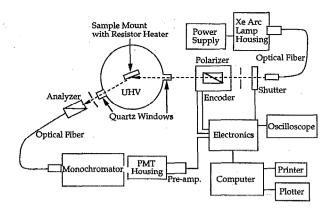$$+ [\Delta(h\nu_i,\Phi_j) - \Delta^c(h\nu_i,\Phi_j)]^2 \}. \quad (5)$$

FIG. 1. Schematic of the experimental setup.

In using a harmonic-oscillator model to express the dielectric function as described in Eq. (4), this MSE function is minimized by varying the parameters of each oscillator.

In case a model layer contains more than one constituent, the Bruggeman effective-medium approximation[18] (EMA) is employed to calculate the effective optical constants of the mixed layer. It can be expressed as

$$f_A \frac{\epsilon_A - \epsilon}{\epsilon_A + 2\epsilon} + f_B \frac{\epsilon_B - \epsilon}{\epsilon_B + 2\epsilon} = 0, \quad (6)$$

where ϵ is the effective dielectric function of the mixed layer. The values of ϵ_A and ϵ_B are the dielectric functions of the material A and B, respectively, and f_A and f_B are the relative volume fractions. This is based on the assumption of a homogeneous mixture and a random-aggregate spherical microstructure (e.g., a GaAs layer with voids).

Associated pseudoquantities can be derived from $\langle\epsilon\rangle$ data, such as the following: Pseudorefractive index:

$$\langle\tilde{n}\rangle^2 = (\langle n\rangle + i\langle k\rangle)^2 = \langle\epsilon_1\rangle + i\langle\epsilon_2\rangle, \quad (7)$$

$$\langle n\rangle = \left(\frac{\langle\epsilon_1\rangle}{2} + \frac{1}{2}\sqrt{\langle\epsilon_1\rangle^2 + \langle\epsilon_2\rangle^2}\right)^{1/2}, \quad (8)$$

$$\langle k\rangle = \left(-\frac{\langle\epsilon_1\rangle}{2} + \frac{1}{2}\sqrt{\langle\epsilon_1\rangle^2 + \langle\epsilon_2\rangle^2}\right)^{1/2}. \quad (9)$$

Normal-incidence pseudoreflectance:

$$\langle R\rangle = \frac{(\langle n\rangle - 1)^2 + \langle k\rangle^2}{(\langle n\rangle + 1)^2 + \langle k\rangle^2}. \quad (10)$$

Pseudoabsorption coefficient:

$$\langle\alpha\rangle = 4\pi\langle k\rangle/\lambda. \quad (10')$$

III. EXPERIMENT

The experimental setup is shown in Fig. 1. A rotating-polarizer ellipsometer (RPE) was attached to the ultra-high-vacuum (UHV) chamber. Two air-spaced Glan–Taylor polarizers were employed to enhance the ultraviolet transmission. The analyzer azimuth angle A was set to vary with the changes of the measured parameter $\psi(h\nu_i,\Phi_j)$ to minimize the calibration error of the system.[19–21] It was set such that $5° \geqslant A - \psi \geqslant 0°$ and $A_{\min} = 10°$. The monochro-

mator was placed between the fixed analyzer and the photomultiplier tube, for improved ambient light rejection (including the blackbody radiation from the hot sample and holder). The sample was clamped on a resistor-heater plate inside the UHV chamber, which could be rotated and tilted by a rotary drive. The angle of incidence Φ was determined by measuring a known GaAs sample at room temperature. The Φ was treated as a fitting parameter, and the value $\Phi = 74.7° \pm 0.02°$ was obtained. Repeatable angle setting was ensured by two apertures positioned in the entrance and reflected beam paths. Two low-strain, fused-quartz windows[22] were employed. The base pressure of the UHV chamber was typically 1×10^{-9} Torr, and the SE measurements were carried out without arsenic overpressure.

The sample surface preparation was designed to reduce, as much as possible, the overlayer on the GaAs substrate, so that the measured pseudodielectric functions $\langle \epsilon \rangle = \langle \epsilon_1 \rangle + i \langle \epsilon_2 \rangle$ would more accurately represent the intrinsic bulk response ϵ. The method of wet-chemical etching has been proven to be a good cleaning procedure for semiconductors.[23,24] However, this method was not suitable for in situ measurements of GaAs inside the vacuum chamber. In Ref. 9 a GaAs sample was wet-chemically etched and then placed into the vacuum system. But SE measurements showed that the sample in the vacuum was covered by a reoxidation overlayer. In our experiment, an arsenic-capped, MBE-grown GaAs sample was employed. The arsenic was deposited on the surface immediately after the material was grown in the MBE chamber. It protected the sample surface from being oxidized in air, so that it could be safely transported to the measurement chamber.

Before the SE measurement, the As-capped sample was heated in UHV up to ~ 350 °C for about 10 min. A very clean and smooth surface was obtained after the arsenic coating evaporated. Figure 2 shows a comparison of the pseudodielectric functions of GaAs at room temperature from our measurements and from the measurements after wet-chemical etching by Aspnes and Studna in Ref. 24. The results are comparable.

An alternative way of obtaining an oxide-free GaAs surface was to heat the sample up to ~ 580 °C and let the oxide desorb. However, in situ SE showed that the GaAs near-surface region was gradually altered before and during the oxide desorption. A detailed study of GaAs (100) surface changes induced at elevated temperatures, including native oxide desorption, has been reported elsewhere.[10,11]

Temperature was measured and monitored by two thermocouples (TC), one attached between the sample and clamp and one to the heater plate; their readings differed by 10 °C at ~ 400 °C. We will refer to the reading from the heater plate as "nominal" and the other as the "averaged" temperature. An IRCON optical pyrometer with a 0.91–0.97-μm bandpass filter[25] was used to calibrate the nominal temperature in the range of 450–700 °C. The pyrometric measurements were performed through the quartz window assuming an effective emissivity of 0.66 for a polished GaAs surface. As shown in Fig. 3, the calibrated
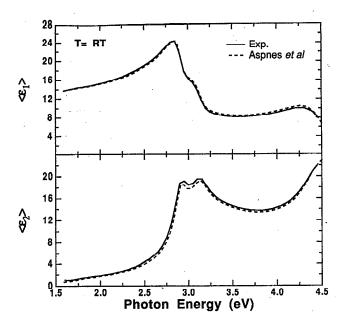

FIG. 2. A comparison of the SE results from two different surface preparation procedures of GaAs: The solid line represents our data from a GaAs surface which was pre-Ar capped; the dashed line refers to the measurements after wet-chemical etching by Aspnes and Studna (Ref. 24).

temperatures from the infrared (IR) pyrometer agreed well with the averaged TC readings up to ~ 520 °C and appeared to be lower as the temperature increased. This indicates a growing temperature gradient between the front and back sample surfaces in the high-temperature range. In the range of 450–700 °C, we will use the IR pyrometer readings as our calibrated temperatures. In the range of RT to 450 °C, the averaged TC readings will be used. Over the entire temperature range, the difference between the actual and measured sample temperatures was estimated to be within 5–10 °C.[25]
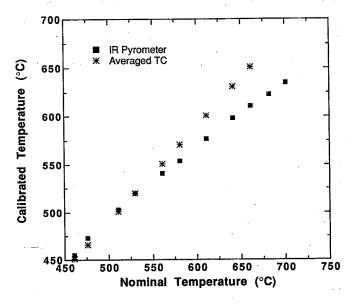

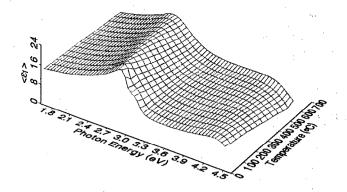FIG. 3. Calibration of the thermocouple reading by an IR pyrometer.

Yao, Snyder, and Woollam   3263

FIG. 4. Real part $\langle\epsilon_1\rangle$ of the pseudodielectric functions of GaAs at elevated temperatures.

IV. RESULTS AND DISCUSSION

A. Optical constants of GaAs at elevated temperatures

Pseudodielectric functions of GaAs at the temperatures ranging from RT to 610 °C are shown in Figs. 4 and 5. The grid line separations represent the actual spacing between data points. In the $\langle\epsilon_2\rangle$ data in Fig. 5, the two closely positioned peaks at ~2.9 and ~3.1 eV, at RT correspond to critical-point transitions E_1 and $E_1 + \Delta_1$, respectively. The separation of these two peaks tends to become less obvious when the temperature is increased. This is due to the increased lattice vibrations which broaden the optical transitions.[6] As temperature increases, these two peaks shift toward lower energy, indicating the decreasing energy threshold of the critical points. A quantitative analysis of the critical-point shifts at elevated temperatures will be discussed in the next section.

SE measurements were made at increments of ~50 °C in the averaged TC reading. Starting at 500 °C, room-temperature SE data were also taken each time, after measurements made at the elevated temperature, in order to check the surface quality. It was found that the sample surface remained smooth and clean until the temperature reached ~577 °C. At this and higher temperatures, the surface became roughened. The surface roughness could be modeled as a top nondense GaAs layer, that is, containing voids. The thickness of this nondense layer and the voids fraction
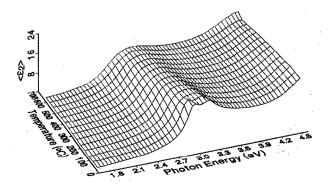

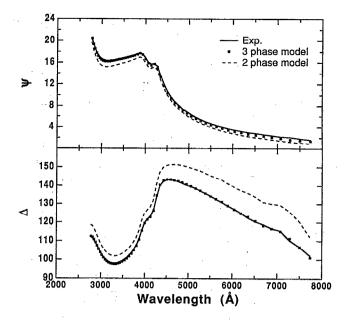FIG. 5. As Fig. 4, but for imaginary part $\langle\epsilon_2\rangle$.

FIG. 6. Room-temperature SE data from a GaAs surface which was heated to 611 °C. The solid line is the experimental data; the dashed line represents a calculation based on a two-phase model (vacuum/substrate); the dotted line is a fit obtained from a three-phase model (vacuum/nondense GaAs/GaAs substrate) assuming a 19.7-Å-thick top layer containing voids and a voids fraction of 0.27.

were calculated by a regression analysis, under the assumptions of the Bruggeman EMA. The thickness of the nondense layer increased with temperature. Figure 6 shows data measured at RT, after heating to 611 °C. These data were fit with the three-phase model: vacuum/nondense GaAs/GaAs substrate, where the thickness and void fraction of the nondense layer were fitting parameters. A very good fit was obtained, with void fraction 0.27 and thickness 19.7 Å. Figure 6 also shows simulated data, for a perfectly smooth, dense, oxide-free surface (two-phase model). Notice the large difference between the two- and three-phase model results, indicating the high sensitivity of SE to only ~20 Å of roughness. Corrections were made mathematically to remove the nondense layer effects for the pseudodielectric functions at 577 and 611 °C shown in Figs. 4 and 5.

We believe this surface roughening is caused by the congruent evaporation of Ga and As at high temperatures between ~577 and ~657 °C.[26] Independent Auger measurements on the heated sample afterward indicated that the stoichiometry of the GaAs sample did not change after being heated to 611 °C.[10]

B. Harmonic-oscillator approximation

The HOA was applied to analyze our SE data in order to explore the critical-point changes as a function of temperature. The pseudodielectric function modeled by the HOA automatically satisfies the Kramers–Kronig dispersion relations.[16,17] A seven-oscillator model, described by Eq. (4), was used to fit the data at each measured temperature, in the range of 2.25–4.45 eV. Among the seven oscillators, four represented the major optical transitions E_1,

3264   J. Appl. Phys., Vol. 70, No. 6, 15 September 1991
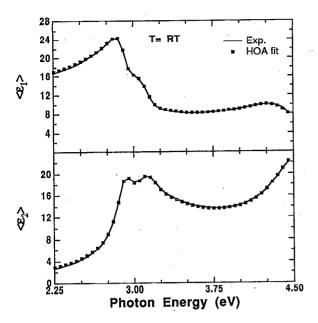
Yao, Snyder, and Woollam   3264

FIG. 7. HOA fit (dashed line) for the pseudodielectric function data (solid line) of GaAs at room temperature, using seven oscillators.

$E_1 + \Delta_1$, E_0', and E_2. Two of the oscillators which were used to describe optical transitions between $E_1 + \Delta_1$ and E_0' did not correspond to any particular critical points. The seventh oscillator with an energy of ~ 10 eV included the effects of all transitions above our spectral range.

Figures 7 and 8 show the pseudodielectric function data at RT and ~ 540 °C, respectively, fitted by the oscillator model. All the parameters A_k, E_k, and Γ_k of each oscillator were allowed to vary except E_7 and Γ_7, to minimize the MSE function in Eq. (5) through a regression analysis. The seven oscillator parameters describing $\langle \epsilon \rangle$ of GaAs at each elevated temperature are given in Table I.
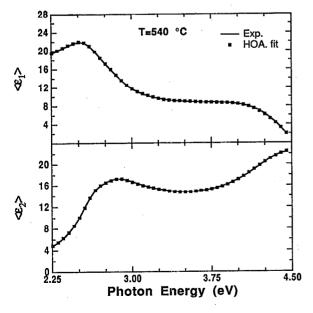

FIG. 8. As Fig. 7, but for $\langle \epsilon \rangle$ data of GaAs at 540 °C.

C. Critical-point temperature dependence

The four center energies E_1, E_2, E_5, and E_6, corresponding to the critical points E_1, $E_1 + \Delta_1$, E_0' and E_2, decrease in value with increasing temperature, indicating an overall downward shift of the critical-point energies. Temperature dependence of the critical points E_1 and $E_1 + \Delta_1$ is shown in Fig. 9. We can see that as temperature increases from RT to ~ 610 °C, the E_1 critical-point energy shifts downward ~ 300 meV. The $E_1 + \Delta_1$ value decreases slightly less over the same temperature range, indicating that the total-energy-band shift is not strictly rigid. Comparing our values of E_1 with the data analyzed by fitting the second-derivative spectrum of ϵ by Lautenschlager et al.,[9] ours agree quite well with theirs between RT and ~ 300 °C, but our measured shifts are slightly smaller at higher temperatures. The values of the critical points E_1 and $E_1 + \Delta_1$ can be least-squares fitted by cubic equations, in the range from RT to 610 °C:

$$E_1(\text{eV}) = 2.927 - 6.349 \times 10^{-4} T$$
$$+ 2.934 \times 10^{-7} T^2 - 1.506 \times 10^{-10} T^3, \quad (11)$$

$$E_1 + \Delta_1(\text{eV}) = 3.132 - 7.131 \times 10^{-4} T$$
$$+ 7.34 \times 10^{-7} T^2 - 5.695 \times 10^{-10} T^3. \quad (12)$$

The E_0' and E_2 critical points are on the boundary, or beyond, the spectroscopic range of our experimental data. Therefore, our data are insufficient for a careful quantitative analysis of these two critical points, as functions of temperature.

It should be pointed out that obtaining critical-point energies via the HOA model, in comparison with the conventional critical-point model[27], is a different approach. It works reasonably well for the two-dimensional (2D) critical-points within the experimental spectral range (i.e., the E_1 and $E_1 + \Delta_1$ in our case).

D. Application to optical thermometry

The temperature-dependent pseudo-optical constants of GaAs, measured at a series of fixed temperatures ranging from 22 to 610 °C, serve as a set of reference functions which can be used to find unknown sample surface temperatures. In this application, the SE acts as an optical thermometer.

We first determine the temperature sensitivity of $\langle \epsilon_2 \rangle$ at various temperatures, by taking the numerical derivative of $\langle \epsilon_2 \rangle$ with respect to T (°C), as shown in Fig. 10. The spectrum of $|d\langle \epsilon_2 \rangle / dT|$ at a fixed temperature represents the relative sensitivity of $\langle \epsilon_2 \rangle$, over the entire spectral range, to changes of temperature. From Fig. 10 the highest sharp peak in each derivative spectrum falls into a spectroscopic window of photon energy ranging from ~ 2.4 to ~ 2.85 eV. The position of each peak in photon energy decreases by about the same amount as the E_1 critical point, as the temperature increases, indicating that the

TABLE I. Values of the oscillator parameters of the seven HOA of the dielectric function of GaAs.

Temp. (°C)	A_1	E_1	Γ_1	A_2	E_2	Γ_2	A_3	E_3	Γ_3	A_4	E_4	Γ_4
22	0.8543	2.9158	0.0948	1.1112	3.1194	0.1487	4.7933	3.3271	0.5154	2.7623	3.9332	0.537
50	0.8314	2.8927	0.0994	1.3502	3.0944	0.1709	4.4728	3.3268	0.506	2.7144	3.9102	0.5253
100	0.8	2.8669	0.1068	1.7259	3.068	0.2001	3.9481	3.3378	0.4939	2.6433	3.8834	0.519
150	0.7805	2.8399	0.1153	2.0358	3.0409	0.2241	3.4848	3.3381	0.477	2.5908	3.8578	0.5142
200	0.7731	2.812	0.1223	2.2802	3.0166	0.2421	3.0827	3.3351	0.4603	2.5569	3.8243	0.5162
250	0.7778	2.7834	0.1323	2.4589	2.9896	0.2559	2.7418	3.322	0.4358	2.5417	3.7998	0.5053
300	0.7945	2.7575	0.1417	2.5719	2.966	0.2666	2.4623	3.3072	0.4169	2.545	3.7683	0.5066
350	0.8232	2.7346	0.1507	2.6193	2.947	0.2749	2.244	3.2906	0.4015	2.567	3.7437	0.5032
400	0.864	2.7113	0.1594	2.601	2.9303	0.2777	2.0869	3.2775	0.3915	2.6076	3.7182	0.5165
450	0.9168	2.6889	0.1709	2.5171	2.9104	0.2818	1.9912	3.2477	0.3845	2.6669	3.6883	0.5201
500	0.9817	2.6671	0.1783	2.3675	2.8923	0.281	1.9567	3.2203	0.389	2.7447	3.6545	0.539
541	1.0586	2.6426	0.1903	2.1523	2.8651	0.2708	1.9834	3.1766	0.3746	2.8412	3.6175	0.5315
577	1.1475	2.6271	0.1983	1.8714	2.8509	0.2602	2.0715	3.1439	0.3793	2.9562	3.5866	0.5383
611	1.2485	2.6172	0.2056	1.5249	2.8453	0.2396	2.2208	3.1294	0.3762	3.09	3.5878	0.5357

Temp. (°C)	A_5	E_5	Γ_5	A_6	E_6	Γ_6	A_7	E_7	Γ_7
22	2.6975	4.449	0.329	6.0257	4.762	0.2933	8.9062	10.006	0.1365
50	2.9167	4.4227	0.3389	6.0844	4.7678	0.2812	8.3987	10.006	0.1365
100	3.2869	4.414	0.3583	6.1867	4.7713	0.2926	7.6737	10.006	0.1365
150	3.6297	4.4021	0.3817	6.286	4.7773	0.3043	7.1339	10.006	0.1365
200	3.945	4.3885	0.4109	6.3823	4.7673	0.3275	6.7113	10.006	0.1365
250	4.2329	4.3815	0.4263	6.4754	4.7695	0.3521	6.4007	10.006	0.1365
300	4.4933	4.3642	0.4525	6.5655	4.7597	0.3689	6.1692	10.006	0.1365
350	4.7264	4.3584	0.4684	6.6525	4.7551	0.4049	5.9946	10.006	0.1365
400	4.9319	4.3484	0.4962	6.7365	4.7399	0.4353	5.8725	10.006	0.1365
450	5.1101	4.345	0.5156	6.8173	4.7304	0.4684	5.8073	10.006	0.1365
500	5.2608	4.3355	0.5444	6.8952	4.7052	0.5052	5.7889	10.006	0.1365
541	5.3842	4.3029	0.5611	6.9699	4.6877	0.5053	5.8245	10.006	0.1365
577	5.48	4.2887	0.5681	7.0415	4.6773	0.5038	5.8897	10.006	0.1365
611	5.5485	4.2834	0.5327	7.1101	5.6956	0.4656	6.0134	10.006	0.1365

temperature sensitivity is mostly associated with the temperature dependence of the E_1 critical point.

An algorithm was developed to compute the dielectric function spectrum at an arbitrary temperature,[28] by linear interpolation of the pseudorefractive indices at two reference temperatures separated by ~ 50 °C. Thus an unknown surface temperature can be determined by fitting the measured data, with temperature as an adjustable parameter.

We have tested this algorithm in our UHV chamber, as well as in a real-time MBE-growth chamber.[8] Shown in Fig. 11, as an example, is a temperature fit of the *in situ* SE data from a GaAs (100) surface measured at ~ 364 °C in our UHV system. The fit temperature (~ 363 °C) and the calibrated TC reading are quite consistent. Generally, the temperatures obtained by SE as an optical thermometer were within ± 10 °C of the conventional temperature measurements.

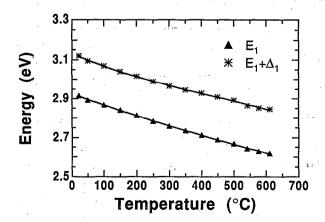As an alternative, linear interpolation of the seven os-

FIG. 9. Temperature dependence of the critical point energies E_1 (solid triangle) and $E_1 + \Delta_1$ (asterisk). The solid lines are polynomial fits for each critical-point energy, respectively, as described by Eqs. (11) and (12).
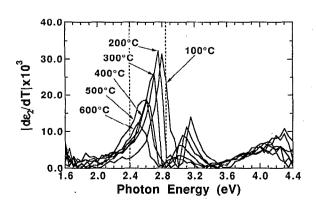

FIG. 10. Temperature sensitivity of $\langle \epsilon_2 \rangle$ at different photon energies. The two vertical dashed lines indicate a spectroscopic window containing the highest sensitivity peaks from each fixed temperature.
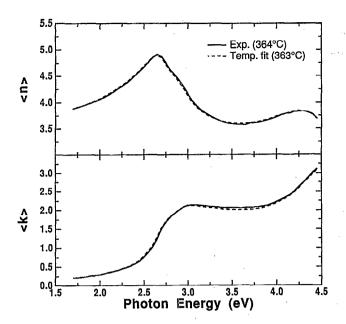
3266   J. Appl. Phys., Vol. 70, No. 6, 15 September 1991

Yao, Snyder, and Woollam   3266

FIG. 11. Temperature fit of the *in situ* SE data from a GaAs (100) surface measured at ~364 °C in the UHV chamber. The solid line is the experimental SE data; the dashed line is the best temperature fit.

cillator parameters at two adjacent temperatures also permits computing $\langle \epsilon \rangle$ at an arbitrary temperature. In our case, results from both interpolations were comparable, due to the slow and smooth changes of each oscillator parameter as a function of temperature.

V. CONCLUSIONS

We have presented a set of pseudodielectric functions and the associated pseudo-optical constants of GaAs at elevated temperatures ranging from RT to ~610 °C. A pseudodielectric function measured by SE is the same as the bulk dielectric function, if no surface overlayer or roughness is present. This requirement was met with an MBE-grown GaAs layer, protected by an arsenic cap. The arsenic cap was evaporated at ~350 °C under ultrahigh vacuum, in the measurement chamber, leaving a clean, smooth surface for SE measurements. The RT results were comparable with those reported for the best wet-chemically processed surfaces. This demonstrates the general usefulness of arsenic capping for SE measurements of III-V semiconductors in UHV. Because there was no As overpressure in the chamber, some surface roughening occurred at temperatures above 550 °C, possibly due to congruent evaporation of Ga and As. SE data at these temperatures were successfully fitted with a model which quantitatively accounted for the roughness. The roughness effects were then mathematically removed.

A harmonic-oscillator approximation was used to fit the measured dielectric functions. Good fits were obtained with this simple model, which provides a convenient means of reproducing the GaAs dielectric function at any temperature, by using the temperature-dependent oscillator parameters. In addition, the HOA analysis provided information about band-gap variation with temperature.

As an application of the data base reported here, we have developed an algorithm to compute the optical functions of GaAs at an arbitrary temperature between RT and ~610 °C. Through a regression analysis, the temperature of a GaAs surface can be determined to a reasonable precision. Thus the ellipsometer can be utilized as an optical thermometer to determine the sample surface temperature in a growth chamber.

Note added in proof. We have recently extended the GaAs temperature-dependence measurements to a spectroscopic range of 1.5–5.0 eV, which includes the E_2 critical point. These results will appear in a future publication, together with temperature-dependence measurements of heavily doped GaAs.

[1] D. E. Aspnes, in *Optical Properties of Solids: New Developments,* edited by B. O. Seraphin (North-Holland, Amsterdam, 1976), p. 799.
[2] P. G. Snyder, M. C. Rost, G. H. Bu-Abbud, J. A. Woollam, and S. A. Alterovitz, J. Appl. Phys. **60,** 3293 (1986).
[3] J. A. Woollam, P. G. Snyder, A. W. McCormick, A. K.Rai, D. C. Ingram, and P. P. Pronko, J. Appl. Phys. **62,** 4867 (1987).
[4] S. A. Alterovitz, P. G. Snyder, K. G. Merkel, J. A. Woollam, D. C. Radulescu, and L. F. Eastman, J. Appl. Phys. **63,** 5081 (1988).
[5] F. Hottier, J. Hallais, and F. Simondet, J. Appl. Phys. **51,** 1599 (1980).
[6] M. Erman, J. B. Theeten, N. Vodjdani, and Y. Demay, J. Vac. Sci. Technol. B **1,** 328 (1983).
[7] D. E. Aspnes, W. E. Quinn, and S. Gregory, Appl. Phys. Lett. **56,** 2569 (1990).
[8] B. Johs, D. Meyer, G. Cooney, H. D. Yao, P. G. Snyder, J. A. Woollam, J. Edwards, and G. Maracus, Mater. Res. Soc. Symp. Proc. **216,** 459 (1991).
[9] P. Lautenschlager, M. Garriga, S. Logothetidis, and M. Cardona, Phys. Rev. B **35,** 9174 (1987).
[10] H. D. Yao, P. G. Snyder, and J. A. Woollam, in Proceedings of ICEM-2, 501 (1990).
[11] H. D. Yao, P. G. Snyder, and J. A. Woollam, Mater. Res. Soc. Symp. Proc. **202,** 339 (1991).
[12] S. Adachi, Phys. Rev. B **41,** 1003 (1990).
[13] R. M. A. Azzam and N. M. Bashara, *Ellipsometry and Polarized Light* (North-Holland, Amsterdam, 1977).
[14] D. E. Aspnes, J. Vac. Sci. Technol. **17,** 1057 (1980).
[15] D. E. Aspnes, in *Handbook of Optical Constants of Solids,* edited by E. D. Palik (Academic, New York, 1985), p. 89.
[16] F. Wooten, *Optical Properties of Solids* (Academic, New York, 1972).
[17] M. Erman, J. B. Theeten, P. Chambon, S. M. Kelso, and D. E. Aspnes, J. Appl. Phys. **56,** 2664 (1984).
[18] D. E. Aspnes and J. B. Theeten, Phys. Rev. B **20,** 3292 (1979).
[19] W. Budde, Appl. Opt. **1,** 201 (1962).
[20] P. S. Hauge and F. H. Dill, IBM J. Res. Develop. **17,** 472 (1973).
[21] D. E. Aspnes, J. Opt. Soc. Am. **64,** 639 (1974).
[22] A. A. Studna, D. E. Aspnes, L. T. Florez, B. J. Wilkens, J. P. Harbison, and R. E. Ryan, J. Vac. Sci. Technol. A **7,** 3291 (1989).
[23] D. E. Aspnes and A. A. Studna, Appl. Phys. Lett. **39,** 316 (1981).
[24] D. E. Aspnes and A. A. Studna, Phys. Rev. B **27,** 985 (1983).
[25] S. L. Wright, R. F. Marks, and A. E. Goldberg, J. Vac. Sci. Technol. B **6,** 842 (1988).
[26] C. T. Foxon, J. A. Harvey, and B. A. Joyce, J. Phys. Chem. Solids **34,** 1693 (1973).
[27] D. E. Aspnes, in *Handbook on Semiconductors,* edited by M. Balkanski (North-Holland, Amsterdam, 1980), Vol. 2, p. 109.
[28] The algorithm was programmed by B. Johs of J. A. Woollam Co.